Journal of Structural Geology, Vol. 8, Nos. 3/4, pp. 281 to 290, 1986
Printed in Great Britain

0191-8141/86 $03.00 + 0.00

Thrust-fault mechanics and origin of a frontal ramp

E. G. BOMBOLAKIS

Department of Geology and Geophysics, Boston College, Chestnut Hill, MA 02167, U.S.A.

(*Received* 1 *July* 1984; *accepted in revised form* 29 *August* 1985)

Abstract—Several features of thrust sheets in nonmetamorphic and relatively low-grade metamorphic terrains indicate that the modes of faulting included both gradual and stick-slip types of motion. A first-order quantitative analysis is made of the mechanics of this type of faulting. In the analysis, part of a wedge-shaped thrust belt slips forward over a fault area of length, L, and unit width, W, producing a strain concentration in subhorizontal strata at the front of the growing thrust, where a frontal ramp develops by shear fracturing. Equations for net slip, X, and the conditions for ramping are evaluated with limit equilibrium principles and coupled oscillator theory.

The quantitative analysis takes into account anisotropy resulting from contrasts in competency and facies changes. A special case solution for maximum net slip associated with 'stick-slip' is

$$X = \frac{\sigma LW}{\Sigma k_i}\,[1 - \cos \omega_0 t + (\omega_0/\omega_1)^2(1 - \cos \omega_1 t)],$$

where σ is the stress drop, k_i are spring constants of the strata, ω_0 and ω_1 are natural frequencies of the system, and t (evaluated from another equation) is the time for net slip. The spring constants and natural frequencies can be evaluated from seismic and stratigraphic data.

A preliminary solution for piggy-back thrusting indicates that ramp spacing can be systematic and that it depends upon the thickness of the deforming package, the elastic parameters of the deforming package, the slope of the topographic surface, and the stresses along the trailing edge of the package.

INTRODUCTION

FUNDAMENTAL differences of interpretation exist between current models of entire wedge-shaped belts. Elliott (1976a) concluded from his model that gravitational forces are dominant in the emplacement of entire thrust sheets; i.e. that horizontal tectonic compression is not necessary for the formation of thrust belts. He also concluded that horizontal compression could dominate only in the frontal zone or toe of a deforming wedge (Elliott 1980). The conclusions of Chapple (1978) were nearly the opposite: horizontal compression can play a major role, and a topographic slope is neither a necessary nor sufficient condition for the formation of a thrust belt, whereas a critical topographic slope can result from compressive flow within the belt. The Stockmal (1983) model and the Davis *et al.* (1983) model also reflect important differences of interpretation. Some are discussed by Stockmal (1983, p. 8284), and need not be discussed here, except to note that almost all models assume uniform rheology and isotropy above the sole.

These differences of interpretation indicate that the mechanics of selected portions of thrust belts need to be analyzed quantitatively in terms of geologic/geophysical field data and material properties. Mechanical anisotropy due to stratigraphic layering and competency contrasts has had a profound influence on the style of deformation in foreland thrust zones (e.g. Dahlstrom 1970, Royse *et al.* 1975, Harris & Milici 1977, Price 1981, Dixon 1982). The current strategy therefore is to analyze foreland thrusting in terms of geologic/geophysical field data and material properties, rather than in terms of theories of plate flexure, migrating foredeeps and plate tectonics.

The purpose of this paper is to present preliminary quantitative analyses of several aspects of foreland thrusting encountered in nonmetamorphic and relatively low-grade metamorphic terrains. Attention is focused on a frontal ramp characterized by a low-angle fault within incompetent strata that 'abruptly' cuts obliquely upsection across competent strata, above which the fault resumes its subhorizontal course within another incompetent sequence. This type of ramp, with flats in the incompetent beds, is a fundamental structure encountered in foreland thrust belts (e.g. Verrall *et al.* 1981, Perry *et al.* 1984), and it constitutes a vital clue to the mechanics of low-angle thrusting.

Different mechanical models for low-angle thrusting and the development of a frontal ramp currently are possible (e.g. see Knipe 1985). They accordingly must be considered tentative models, subject to further development when warranted by appropriate tests. The preliminary prototype models presented here are constrained as follows. They take into account mechanical anisotropy resulting from stratigraphic layering and competency contrasts, including facies changes. They also take into account the features of fault motion described in the next section.

CHARACTERIZATION OF FAULT MOTION

Studies of modern faulting demonstrate that fault motion involves stable sliding and stick-slip modes (Kasahara 1981, Raleigh 1982). These modes may or may not have anything to do with friction (e.g. Bombolakis *et al.* 1978), and so it is probably best to describe stick-slip in somewhat more noncommittal terms as a

phenomenon associated with rapid temporary changes in shear resistance, rather than as a phenomenon associated with rapid changes between the coefficients of static and sliding friction, until we know to what extent the faulting is frictional (Elliott 1976b, Bombolakis 1979). The cutout depth of microseismic activity in continental fault zones currently appears to correspond to the onset of greenschist metamorphic conditions at about 300°C (Sibson 1984).

In addition to the studies of modern faulting, there also are a few lines of evidence which indicate that the displacement along major thrusts was intermittent and included both gradual and stick-slip types of motion. Laboratory studies of welded gouge (Friedman *et al.* 1974) are consistent with the interpretation that the types of pseudotachylyte reported along a Himalayan thrust (Scott & Drever 1954) and the Outer Hebrides Thrust zone (Sibson 1975) resulted from seismic faulting. In North America, Bustin (1983) found that anomalously high vitrinite reflectances obtained from the Lewis thrust, the McConnell thrust, the Coleman thrust, and two unnamed thrusts in the Canadian Rockies, are restricted to very narrow films within the shear zones which, considering any reasonable thermal conductivity, indicates that elevated temperatures (360–650°C) were short lived, thereby indicative of paleotectonic stick-slip. Further south, in the Utah–Idaho–Wyoming thrust belt, there is considerable evidence that fault motion proceeded in a stop-and-go fashion, on both the grand scale and the scale of a single thrust system. Thrusting across the entire belt apparently progressed episodically from the hinterland to the foreland (Armstrong & Oriel 1965, Royse *et al.* 1975, Wiltschko & Dorr 1983). A unique feature of this thrust belt is that so many portions of synorogenic conglomerates have been preserved for study. Palynologic dating and structural analysis of synorogenic conglomerates in the Fossil Basin area demonstrate that these conglomerates record an episodic history of displacement on the Absaroka thrust system from pre-mid Santonian to middle Paleocene time (Lamerson 1982, p. 337).

Several lines of evidence also have shown that the Hubbert-Rubey hypothesis in its original form can be ruled out as a viable hypothesis. One of these lines of evidence has received little attention in the literature, and since it is pertinent to the discussion of stable sliding and stick-slip modes, it is discussed briefly here. Rubey & Hubbert (1959, pp. 199–200) originally calculated tentatively that high pore pressures would have had to exist simultaneously over a thrust surface area as large as 25,000 square kilometers. Since the time this calculation was made, hardly any supportive field evidence (hydraulic fractures, breccia-dikes, etc.) of the type described by Sibson (1981) has been reported for exposures of thrust-fault contacts in foreland thrust belts. Gretener (1977) is not fully certain that the 'basal tongues' he has observed in various thrust belts are the result of paleotectonic abnormal pore pressures. Brock & Engelder (1977) showed that the 'basal tongues' in the Buffington window exposure of the Muddy Mountain thrust contact in Nevada are composed of gouge that evidently had been intruded into the hangingwall without the aid of high pore pressure. They were able to show that field aspects of the fault contact are consistent with features associated with stable sliding and stick-slip observed in laboratory experiments. Since then, field evidence against high pore pressure emplacement of both the Keystone and Red Spring thrust plates in Nevada also has been reported by Axen (1984).

Gretener (1972, 1981) proposed a modified version of the Hubbert-Rubey hypothesis in which the fault movements are discontinuous, caterpillar-like, both in time and space. It involves 'rapid' loading by tectonic advance of a thrust sheet beyond a ramp on to a flat, beneath which sedimentary strata are subjected to tectonic and aquathermal overpressuring. A field observation by Winslow (1983) tentatively confirms one prediction of Gretener's hypothesis of tectonic overpressuring. In her study of the southern Andes, Winslow found that extensive clastic dike swarms had been emplaced mainly in the frontal portions of major thrusts. By way of example, however, the Pine Mountain thrust region in the southern Appalachians provides a strong contrast. Harris & Milici (1977) made important detailed maps of extensive fresh roadcuts that penetrated down to the Cumberland Plateau thrust surface and the Ozone decollement. The 'broken formation' and fracture zones just above the fault surfaces demonstrate that the deformation was predominantly brittle, with no clear evidence that high pore pressures had existed. In general the field evidence for high pore pressures is relatively rare in this region (David Wiltschko, personal communication, 1983). It also is apparently rare in the Central and Northern Appalachians (Peter Geiser, personal communication, 1984).

In the case of the modern Taiwan belt system, moderately high pore pressures have been documented in the western third of the wedge (Davis *et al.* 1983). Elsewhere in the belt, pore pressures have been inferred principally from sonic logs, which frequently are used to infer the existence of overpressured shales and clays. This inference is uncertain without additional data because sonic logs actually reflect formation density and porosity, not pore pressure. The permeability of some shales and clays, such as those containing sodium montmorillonite, is so low that some so-called 'overpressured' shales are shales that simply have not reached normal consolidation due to very low permeability. A clue that this condition may exist occurs when the drill penetrates an interbedded sand having normal formation pressure. Consequently, the pore pressure distribution in the Taiwan belt will have to be defined by additional drilling and geophysical data. Some of the current geophysical data, however, are particularly important for inferring fault motion modes. Figure 11 of Davis *et al.* (1983, p. 1163) shows hypocenters of small earthquakes (e.g. magnitudes in the 2–4 range) distributed through part of the toe region. These indicate that some of the displacements are being achieved by stick-slip, even in this part of the Taiwan belt.

This discussion has treated only a few key aspects of the topic of fault motion, principally from a mechanistic viewpoint. Taken together with the geometric/kinematic aspects discussed by Dahlstrom (1970), Royse *et al.* (1975) and Boyer & Elliott (1982), the following characterization of fault motion can be made with respect to the 'staircase' structure of foreland belts illustrated by Roeder *et al.* (1978), Price (1981) and Dixon (1982). Fault displacements within the unmetamorphosed and relatively low-grade metamorphic terrains probably are discontinuous, caterpillar-like, both in time and space, and include stable sliding and stick-slip modes.

Several styles of deformation are possible if stable sliding and stick-slip modes occur in the frontal zone of a growing low-angle thrust. The possibility treated in this paper is that a frontal ramp begins to form by shear fracture in response to episodic high strain-rate loading of competent strata in the prospective ramp region. A model of this process incorporates ramp features that can be compared or contrasted with field and experimental observations which depend on the origins of ramps. This topic, therefore, is considered in the next section before proceeding with the quantitative analyses.

ORIGINS OF FRONTAL RAMPS

The origins of frontal ramps have not been established yet. A brief review of a few possibilities is discussed here, beginning with Fisher & Coward (1982). They reported field evidence indicating that some ramps in the Heilam sheet of the Moine thrust zone originated during asymmetric folding (see their Fig. 19, p. 310). Two of the diagnostic features discussed by the authors are the amount of strain and style of folding in the footwall. The maximum value of layer parallel shortening measured by the authors is 33%, which they suggest was a critical value for the rocks, a value above which shortening may have taken place by buckling and then by propagation of the thrust across the beds.

The amount and style of penetrative deformation in the Moine district, however, contrasts with the usual lack of penetrative deformation reported for the Southern Canadian Rocky Mountain foreland belt (Price 1973) and the Utah–Idaho–Wyoming thrust belt (Rubey & Hubbert 1959, Wiltschko & Dorr 1983), if we discount such features as locally penetrative, axial planar cleavage developed in some of the shales, and pressure solution effects in some of the limestones. Strains reported for ramp regions of the McConnell thrust (Spang & Brown 1981, Spang *et al.* 1981) are only about 5%, quite different from the Heilam example.

Unique rock deformation experiments by Morse (1977) indicate that strains in the footwall of a ramp can be very small, and should be appreciably smaller than in certain portions of the hangingwall when a frontal ramp exists prior to folding in the ramp region. Scaling problems naturally exist when relating laboratory experiments to field examples, and so it is worth noting two relevant facts. First, the classic Rangely oil field experiments (Raleigh *et al.* 1976) comprise a well-documented case in which predictions based on laboratory faulting experiments were applied successfully in the field, despite a difference in scale of four to five orders of magnitude between field experiment and laboratory experiment. Secondly, Morse's experimental results are consistent with the mode 3 style of deformation reported by Serra (1977), who mapped numerous small-scale ramps in various thrust belts of the U.S.A. and Canada. The mode 3 style is characterised by curved reverse faults formed in the hangingwall of the ramp region. This mode was observed only when the bed thickness approximately equaled ramp height, as in Morse's experiments.

On a larger scale, it appears that many ramps do predate the folds (e.g. Butler 1982). Thus, one of the key elements for deducing the origin of a frontal ramp is the strain and fracture condition of the footwall of the ramp, as implied by the geometric-kinematic models of Douglas (1950), Dahlstrom (1970), Gretener (1972), Boyer (1978), Boyer & Elliott (1982), Bombolakis (1982) and Suppe (1983). Another key element is whether a frontal ramp is genetically related to preexisting basement structures. Wiltschko & Eastman (1983) found that such structures theoretically could localize stress concentrations in overlying strata. They suggested that these stress concentrations might control the location of some frontal ramps. The cross-sections of Dixon (1982), however, show that some sort of systematic spacing exists between frontal ramps in the Utah–Idaho–Wyoming thrust belt, over large areas where the underlying Cambrian–Precambrian contact is smooth, almost planar. This situation is illustrated by the data in Table 1, even though the actual spacing that developed kinematically between sequentially developed frontal ramps has not been determined yet.

Table 1. Spacing between major frontal ramps of the Crawford (C), Absaroka (A) and Hogsback (H) thrusts in cross-sections 29, 30 and 31 of Dixon (1982), Utah–Idaho–Wyoming thrust belt

Section	* Present deformed state			* Palinspastically restored state		
	From C to A	From A to H	(C–A)/(A–H)	From C to A	From A to H	(C–A)/(A–H)
29	25.0 ± 1.0	28.0 ± 0.5	0.89 ± 0.04	67.0 ± 1.5	44.5 ± 1.0	1.51 ± 0.05
30	28.0 ± 1.0	28.0 ± 0.5	1.00 ± 0.04	81.0 ± 1.5	48.5 ± 1.0	1.67 ± 0.05
31	24.5 ± 1.0	30.5 ± 0.5	0.80 ± 0.04	100.0 ± 2.0	50.0 ± 1.0	2.00 ± 0.06

* In each case, ramp spacing is measured in kilometers along the sole in the foreland direction. The piggy-back sequence of the thrusts listed in this table is from C to A to H. The actual ramp spacing during sequential development of the major ramps has not been determined yet. Cross-sections 29, 30 and 31 are mutually subparallel, oriented perpendicular to the strike of the belt, and spaced approximately 10 km apart along strike. They extend westward from the Kemmerer region of Wyoming into Utah (see locations and configurations in Dixon 1982).

Wiltschko & Dorr (1983) report that their palinspastic analysis of the two Royse *et al.* (1975) cross-sections across this belt indicates that the spacing decreases in the direction of tectonic transport. Peter Geiser (personal communication, 1984) found evidence for just the opposite relationship in certain parts of the Appalachians. A theory for the origin of these frontal ramps accordingly must account for variations in ramp spacing.

The two prevalent thrust propagation models for the sequence of thrusting (Elliott & Johnson 1980, Butler 1982) are (1) *Overstep:* subsequent thrusts propagated backwards towards the hinterland and (2) *Piggy-back:* thrusts propagated towards the foreland. Good examples of large scale overstepping are rare, whereas the piggy-back sequence is well documented for the Helvetic nappes (Trümpy 1973, Ramsay 1981), the northern part of the Moine thrust zone (Elliott & Johnson 1980), and the Southern Canadian Rocky Mountain foreland belt (Dahlstrom 1970, Price 1981). It also is well documented in the Utah–Idaho–Wyoming belt (Royse *et al.* 1975, Dixon 1982, Lamerson 1982, Wiltschko & Dorr 1983). Overstepping in this belt seems to be restricted to some subsidiary structures associated with major thrusts; e.g. the break-back sequence of imbricates associated with the frontal ramp of the Hogsback thrust in the Kemmerer region of Wyoming (Delphia & Bombolakis 1985).

Mandl & Shippam (1981) published an incomplete but potentially applicable analysis of imbrication in the break-forward mode. A finite element technique was employed to model the movement of an isotropic brittle thrust plate along horizontal plastic substrata. Successive imbrication was postulated to propagate from the rear towards the foreland. Their comparison of about fifty numerical model solutions indicates that the spacing d_r between successive imbricates ($r = 1, 2, 3, \ldots$) for the break-forward case is given by

$$d_r = l_0(1 - \beta)\beta^{r-1}$$

where β is a dimensionless parameter and l_0 is the length of an intact segment of the thrust plate just prior to progressive imbrication. Mandl and Shippam's solutions indicate that β has a value between 0.75 and 0.9. Consequently, this equation shows that the spacing between imbricates decreases in the direction of tectonic transport, a prediction that can be tested.

The origins of frontal ramps constitute one of the principal keys for deciphering the actual mechanics of thrust belts. But thus far, no published quantitative analysis of the mechanics of piggy-back thrusting accounts for the origin and spacing of frontal ramps. Therefore, first-order quantitative analyses of this problem are presented in the next three sections.

STICK-SLIP MODEL FOR LOW-ANGLE THRUSTING

The geometry of frontal ramps that pre-date folding in the ramp region, with relatively small strains in ramp footwalls, indicates a mechanism that will be shown to be consistent with observations of presently active faults, where 'tectonic' compression induces premonitory basal creep leading to a rapid transient stress drop along the fault horizon. The effects of such stress drops can be calculated with the impulse-momentum theorems of physics, even though the physico-chemical basis required for an understanding of the stress drops has not been established yet (Bombolakis 1981).

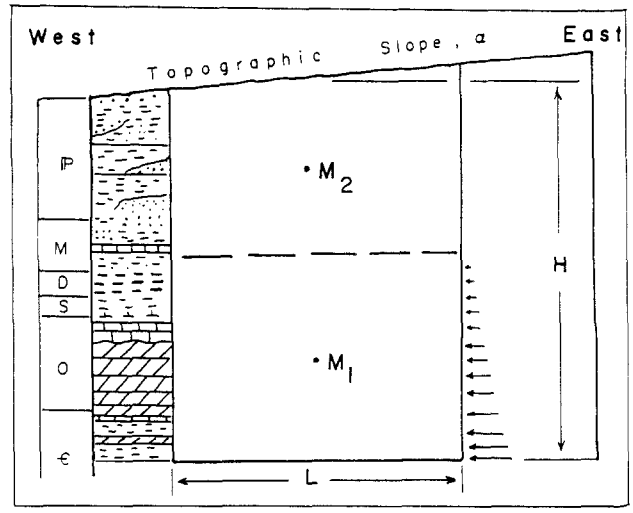

Fig. 1. Geologic cross-section just prior to formation of a frontal ramp. Stratigraphy is shown in prospective ramp region, where subsequent ramp height is measured between L and the dashed line. L is the length of the fault block segment that undergoes westward stick-slip, producing a strain concentration in the prospective ramp region. See text.

In earthquake mechanics (Kasahara 1981), the 'rupture length' L is that segment of a fault surface that undergoes a stick-slip type of displacement. L ordinarily is not the same as the total length of the fault, and it usually does not have a simple relation to the concept of tip-line defined by Elliott (1976b) and other workers (e.g. Hossack 1983). What we consider here is that 'tectonic' compression and the induced stress drops may cause various parts of a thrust sheet to slip forward at different times in the stick-slip mode. When this phenomenon occurs within the frontal zone of a growing low-angle thrust, then a frontal ramp might begin to form by shear fracturing in response to episodic high strain rate loading of the potential ramp region.

The picture for quantitative analysis is illustrated in Fig. 1. It is a geologic cross-section of unit width W perpendicular to the diagram, just prior to ramp formation. The stratigraphy in the potential ramp region is shown at the western end of the cross-section. For convenience, suppose Fig. 1 represents a schematic version of the incipient Cumberland Block in the southern Appalachians, and that the direction of tectonic transport is due West. The tip-line of the Pine Mountain fault then would be located at the western end of L. This tip-line eventually becomes a branch-line when the ramp is formed, following stick-slip of the fault block segment defined by L, H and topographic slope angle α. The dashed horizontal line is a stratigraphic level just above the Chattanooga shales, within which the Pine Mountain fault resumes its course westward after ramping.

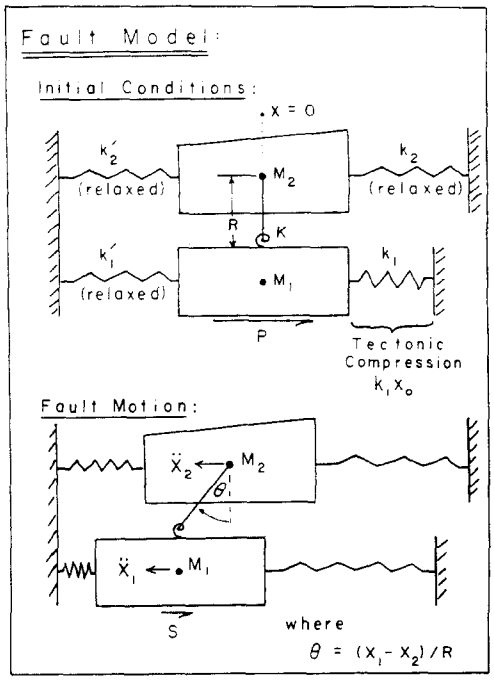

Fig. 2. Damped coupled oscillator model of stick-slip of the fault block segment in Fig. 1.

The mean and deviatoric stresses are not shown in Fig. 1. A simplified version of the stresses is needed to facilitate explanation of the model. For this reason, we will assume that the 'tectonic' component of the stresses has approximately the distribution shown by the arrows, even though 'tectonic' stresses actually extend higher in the section in the real situation. Length L represents the 'rupture length' when stick-slip occurs, and M_1 plus M_2 represents the total mass per unit width of the fault block segment. M_1 is the mass of that part of the block with a thickness equal to subsequent ramp height, and M_2 is the mass of overlying strata involved in the stick-slip event because of mechanical coupling between M_1 and M_2.

Stick-slip of the fault block segment therefore is mathematically equivalent to the type of damped coupled oscillator shown in Fig. 2. This model is not designed to illustrate the detailed variation of stress throughout the fault block segment. Rather, two of its basic objectives are (1) to illustrate the effects of 'tectonic' loads and (2) to provide a practical means of making preliminary quantitative analyses of the effects of fault slip. For example, the elastic constants k_1, k_1', k_2, k_2', including torsion constant K, can be calculated from seismic and stratigraphic data. These elastic constants take vertical and horizontal facies changes into account in a quantitative manner, as will be explained after we discuss the dynamics of the system.

The basal shear stresses are not uniformly distributed along the fault surface of this prototype model, nor along a comparable segment of an actual fault. They vary in a manner yet to be determined; hence the use of average P and average S in Fig. 2, which can be calculated from the force equations. The situation here is similar with respect to quantitative fault models in seismology. For many years, seismologists have modeled earthquake fault motion by a uniform slip or a uniform stress drop over the fault plane, whereas the analysis of barrier and asperity models is still in a preliminary stage (Aki 1984). Consequently, until the new asperity and barrier models are adequately developed quantitatively, the advisable way to presently evaluate the model in Fig. 2 is to test it in terms of the results of focal mechanism studies. Therefore, let us proceed with the analysis of Fig. 2 from this point of view.

Compression of the k_1-spring in the upper diagram of Fig. 2 is caused by creeping motion along the sole, east of the fault block segment in Fig. 1. If the ensuing creep displacement at the base of M_1 is small compared to L, then the other springs in Fig. 2 will remain in an almost tectonically relaxed state during premonitory compression of the k_1-spring. When this compression reaches the critical value shown, the 'peak' shear resistance P of the incompetent bed is overcome at the base of M_1, producing a transient stress drop from P to S, resulting in the stick-slip motion illustrated in the lower diagram.

M_1 undergoes an acceleration $\ddot{X}_1$. It activates the torsion spring, which causes the overlying strata to undergo an acceleration of $\ddot{X}_2$. X_1 is the displacement coordinate of M_1 and X_2 is the displacement coordinate of M_2, with R equal to the radius of gyration of M_2. The equations of motion are

$$M_1\ddot{X}_1 + (k_1 + k_1')X_1 + (K/R^2)(X_1 - X_2) = (P - S)LW \quad (1)$$

$$M_2\ddot{X}_2 + (k_2 + k_2')X_2 + (K/R^2)(X_1 - X_2) = 0. \quad (2)$$

Equations (1) and (2) comprise a nonhomogeneous set of simultaneous second order differential equations. A special case solution illustrates some of the physical implications and the model's compatibility with the results of focal mechanism studies. The special case is $M = M_1 = M_2$, with $k = k_1 = k_1' = k_2 = k_2'$.

The solution for basal fault slip under these conditions is

$$X_1 = \frac{(P - S)LW}{4k}\left[1 - \cos\omega_0 t + (\omega_0/\omega_1)^2(1 - \cos\omega_1 t)\right] \quad (3)$$

where

$$\omega_0 = \sqrt{2k/M}; \quad \omega_1 = \sqrt{2(k + K/R^2)/M}.$$

Equation (3) shows that the fault displacement X_1 is directly proportional to the stress drop $(P - S)$ and rupture length L, where W is the unit width of the fault surface. This stress drop is proportional to the seismic stress drop calculated in earthquake seismology (see Kasahara 1981, eqn 6.14 of pp. 140–141, eqn 6.23 of p. 149). Seismic stress drops have been found to be (1) nearly constant for small earthquakes, (2) nearly independent of source dimensions and (3) the fault displacements have been found to vary nearly linearly with rupture length in the larger earthquakes where they are more easily measured (Scholz 1982). The model, therefore, is consistent with the results of focal mechanism studies.

Equation (3) shows that the fault displacement also is dependent on the natural frequencies of the system,

where ω_0 is the fundamental frequency and ω_1 is the first harmonic, both of which can be calculated from seismic and stratigraphic data. For example, in Fig. 2, k_1' is the sum of the spring constants of the strata cut by the frontal ramp when the strata have been subjected to the same strain (see Den Hartog 1956, p. 36). The spring constant of each bed can be calculated from the thickness and Young's Modulus of the bed, as will be shown in a subsequent publication. This means that the model not only takes into account anisotropy due to contrasts in competency and facies changes, it also takes into account lateral changes of bed thickness. The importance of this result is indicated by the fact that miogeoclinal strata of the Utah–Idaho–Wyoming thrust belt thicken westward away from the foreland.

The net slip of a stick-slip event can be determined from the duration time of stick-slip motion. Towards the end of a stick-slip event, the velocity of the lower block of competent strata decreases to zero, whereas the motion of the overlying strata continues in an oscillatory phase. This phase persists until damping terminates the ground motion. Consequently, differentiating equation (3) once with respect to time, and setting the resulting velocity equation equal to zero, the duration time equation is found to be

$$\cos \omega_0 t = \pm\sqrt{1 - (\omega_0/\omega_1)^2 \sin^2 \omega_1 t}. \quad (4)$$

Therefore, if we calculate the natural frequencies from seismic and stratigraphic data, we can solve eqn (4) for the duration time and substitute it into eqn (3) to determine the net slip. This slip imposes a strain concentration on the potential ramp region that could lead to shear fracturing and ramp development.

The displacement equation for the overlying strata during stick-slip has a form very similar to that of eqn (3); namely,

$$X_2 = \frac{(P - S)LW}{4k} \cdot [1 - \cos \omega_0 t - (\omega_0/\omega_1)^2(1 - \cos \omega_1 t)]. \quad (5)$$

It shows that the horizontal motion of the topographic surface initially lags behind the seismic fault displacement along L by an amount

$$X_1 - X_2 = \frac{(P - S)LW}{2k} \cdot (\omega_0/\omega_1)^2 \cdot (1 - \cos \omega_1 t). \quad (6)$$

The difference in displacement varies from zero at the beginning of stick-slip (at time $t = 0$) to a specific value at the end of a stick-slip, determined by time t in eqn (4). The oscillatory motion of the overlying strata then transforms to a phase with a frequency

$$\omega_n \simeq \sqrt{(2k + K/R^2)/M}. \quad (7)$$

which enables the stick-slip fault model to be tested with seismic measurement techniques.

Equations (1)–(7), of course, were obtained for the simplified version of the problem shown in Fig. 1. The equations for the more realistic situation, in which 'tectonic' stresses extend higher in the section, are theoretically of the same form but much more complicated. Therefore, the general solution, in which all the parameters may vary, will be presented in a subsequent publication.

SHEAR-FRACTURE ORIGIN OF A FRONTAL RAMP

The geometry of frontal ramps that pre-date folding in the ramp region, with relatively small strains in ramp footwalls, suggests the possibility of a shear fracture origin due to elastic strain concentrations imposed on the potential ramp region by stick-slip faulting. This possibility will need to be tested in various ways to determine whether it constitutes a viable hypothesis. Recent seismic case histories reveal that stick-slips called 'characteristic earthquakes' apparently recur along nearly the same rupture length with nearly the same net slip (Coppersmith & Schwartz 1984, Schwartz & Coppersmith 1984). Several effects should be produced in the potential ramp region in this case. For example, if the elastic strains are imposed sequentially on the potential ramp region by recurring stick-slip along L in Fig. 1, then part of these strains should be converted to permanent strains early in the deformation sequence; e.g. by twin gliding of calcite grains in a carbonate member of the sedimentary package.

A characteristic feature of plastic deformation is that work hardening occurs with an increase in both the elastic limit and the yield point, with relatively little change in the elastic modulus in the loading direction, provided recurring deformations follow the same stress deformation path (Nadai 1950, p. 19), as illustrated by the sequential deformation tests on Salem limestone by Donath (1968). We therefore have the important possibility that the development of a through-going shear fracture, forming a frontal ramp, can be estimated quantitatively with limit equilibrium principles, using appropriate elastic stress–strain relations and Coulomb shear fracture criteria. Inspection of the Griggs–Handin rock deformation diagrams (Hobbs *et al.* 1976, fig. 1.29) indicates that the total strain of intact rock in the ramp footwall should be less than 8%, and certainly not more than 10% if pressure solution effects are not pervasive.

This working hypothesis is consistent with the results of Spang *et al.* (1981). They calculated average strains of 5% from calcite and dolomite lamellae measurements in ramp regions of the McConnell thrust plate. The maximum principal strain was found to be subparallel to bedding, and parallel to the direction of tectonic transport. Similar results have been obtained for host rock of the Maynardville limestone in the Pine Mountain thrust plate (D. Wiltschko, personal communication, 1985).

Therefore, returning to Fig. 1, let us now consider the effective stresses generated in the potential ramp region by stick-slip faulting. They can be calculated, but not in the usual manner. To illustrate this important point, consider for a moment two identical, confined, permeable wackestone test specimens: one containing pore

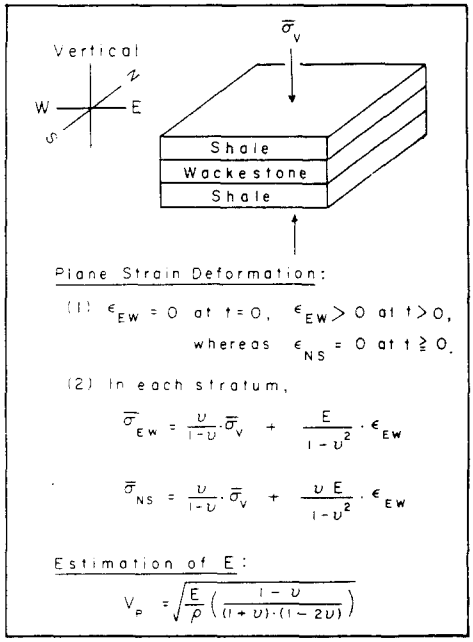

Fig. 3. Stick-slip induced tectonic elastic strain ϵ_{EW} and corresponding stresses in a small portion of the sedimentary package of the prospective ramp region. The strains are the same in each bed of this example, but the effective stresses differ according to respective values of Young's modulus E, Poisson's ratio ν, and pore pressure P in the wackestone. The effective vertical stress in the shales equals the total overburden pressure. V_p = compressional wave velocity, ρ = density and t = time.

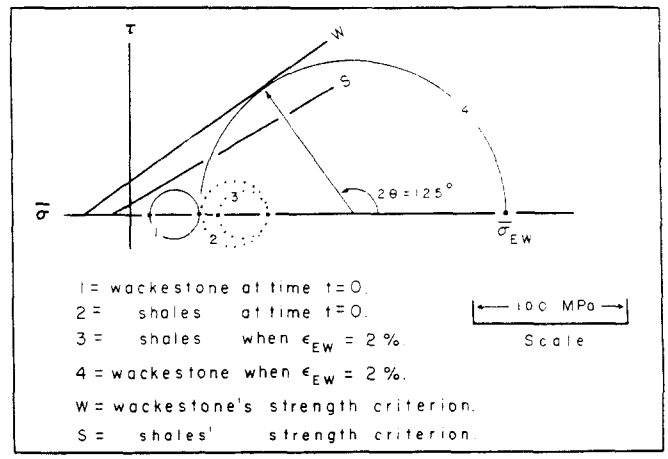

Fig. 4. Example of stress history leading to selective shear fracturing in the prospective ramp region of Fig. 1. Pore pressure in the wackestone is 40 MPa in this example. See Fig. 3 and text.

fluid, the other containing no pore fluid. Compress each specimen with the same elastic strain. The effective stress will be practically the same in both specimens, even though the pore pressures will be very different.

Next, imagine a permeable wackestone bed under moderate pore pressure between two shale beds in the potential ramp region. Two important special cases are (1) that the wackestone is laterally extensive and (2) that the wackestone is not laterally extensive due to permeability barriers associated with facies changes or pinch outs. Hydraulic fracturing, instead of shear fracturing, could occur in the second case because the tectonic strain imposed by stick-slip faulting increases both the pore pressure and the effective stress. For case (1), however, the pore pressure increase is highly transient in the potential ramp region. This pore pressure increase actually represents a pressure pulse due to the high strain rate at which the tectonic strain is imposed. Theoretically, this pressure pulse starts to travel with a speed between the compressional wave velocity of the pore fluid and that of the pure matrix. Hence, the net increase in pore pressure is negligible in case (1) because the tectonic strain is concentrated in the potential ramp region, whereas the pore pressure pulse is damped out throughout the entire wackestone bed in a very short period of time. The following analysis deals with this particular case.

Stick-slip along L in Fig. 1 imposes an elastic tectonic strain ϵ_{EW} under plane-strain conditions at the western end of M_1. A very small part of that sedimentary package is pictured in Fig. 3 as a competent bed of wackestone sandwiched between two incompetent shale beds. The imposed state of strain is nearly the same for each of these strata. It induces an E–W compressive stress $\bar{\sigma}_{EW}$ and a N–S compressive stress $\bar{\sigma}_{NS}$, as indicated by the equations shown under item (2) in Fig. 3. Therefore, even if the effective overburden pressure $\bar{\sigma}_V$ were practically the same in each bed, the states of stress could differ appreciably during tectonic straining, depending on the values of Young's modulus E and Poisson's ratio ν.

For reasons discussed by Nelson (1981), E and ν should not be calculated directly from standard laboratory test data. Therefore, consider the P-wave velocity equation at the bottom of Fig. 3. It shows that Young's modulus is proportional to the square of the velocity. Comparisons of P-wave velocities of 'weak' shales and competent strata (e.g. Nettleton 1940) show that E can be 10 to 20 times smaller for 'weak' shales. Consequently, to illustrate the deformational response of the strata in Fig. 3, the modulus of the shales is taken to be 10 times smaller than the wackestone's modulus. Let $E = 10^4$ MPa for the wackestone. Poisson's ratio is chosen arbitrarily at 1/3 for the shales and 1/5 for the wackestone, in lieu of the fact that legitimate values are not yet available in the literature.

The deformational response of the strata in the prospective ramp region is illustrated with the Mohr diagram analysis in Fig. 4, for a depth of 3.5 km, just a short distance above the sole fault in the Cambrian shale sequence in Fig. 1. Figure 4 shows how limit equilibrium principles could be applied at various stratigraphic levels in the prospective ramp region. The overburden stress in the shales in Fig. 3 is about 80 MPa, corresponding to the depth of 3.5 km chosen for this example. The shear fracture strength criterion for the competent wackestone bed is based on representative values listed by Handin (1966). The shear strength criterion for the two shales, whatever it may be, is graphed at a lower position in Fig. 4. The dotted Mohr circles represent specific stress states in the shales. The solid-line Mohr circles correspond to effective stresses developed in the wackestone when the pore pressure in the wackestone is a little larger than that

calculated from the normal hydrostatic fluid pressure gradient with depth.

The Mohr circles at time $t = 0$ represent the approximate nontectonic states of stress in the shales and wackestone at 3.5 km depth. But during tectonic straining, the E–W compressive stress increases by a greater amount in the stronger bed than in the shales. A striking result is that the 'weak' shales actually can become mechanically more stable during tectonic straining. The smallest dotted Mohr circle in Fig. 4 illustrates this situation. This Mohr circle represents the state of stress in the shales when the tectonic strain has increased to about 2%, whereas the largest solid-line Mohr circle represents the limiting state of stress in the wackestone for the same amount of strain. Consequently, it is the wackestone that undergoes preferential shear fracture, even though their triaxial strengths may or may not differ much.

Similar results are obtained in Fig. 4 if the wackestone is assumed to have no pore pressure. The principal difference in this case is that the critical value of tectonic strain for shear fracture of the wackestone is closer to 4% than to 2%. The implication here is that the throughgoing shear fracture, that forms the ramp, would not have propagated spontaneously as a single rupture event during the last major stick-slip along L in Fig. 1 when significant departures from the normal hydrostatic fluid pressure gradient with depth exist in several units within the relatively competent sequence cut by the frontal ramp. The implication in this case is that shear fracture development of the frontal ramp would have proceeded in stages during the history of recurring stick-slip. A consequence that can be tested by field studies is that specific smaller scale fracture/fault systems would have been developed within several stratigraphic units in the footwall of the ramp. A comparison of the detailed cross-sections of Serra (1977) with those of Suppe (1983) illustrates several possibilities.

SPACING OF FRONTAL RAMPS

An important geometric-kinematic model of thrust fault propagation based on field studies and balanced cross-sections is shown in Fig. 5. A brief review of this model is given by Hossack (1983). The kinematics are as follows. The basal décollement, represented by the thick solid line on the right, has grown to the point denoted 'Trailing branch line', where a frontal ramp develops across a block of competent strata. The upper plate then moves over the frontal ramp to form the rootless anticline shown. The upper plate presumably becomes locked temporarily in position, and the basal décollement subsequently propagates as a 'developing thrust' over length L. A new frontal ramp then forms at the location shown by the small arrows, where L now represents the spacing between the two frontal ramps. The preliminary hypothesis introduced here is that stick-slip occurs along L, so that L also is a seismic rupture length of the sole fault.

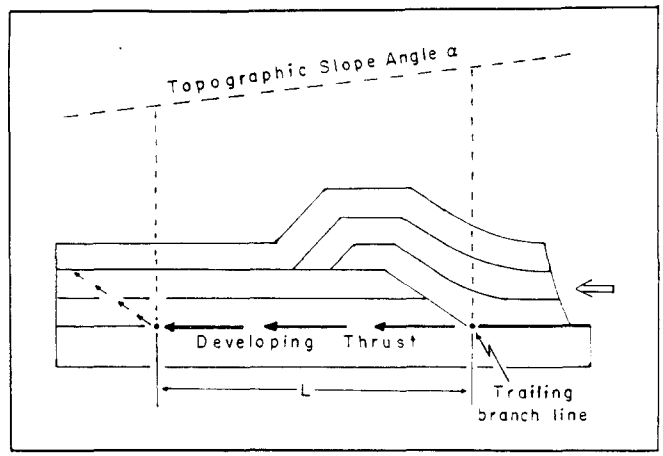

Fig. 5. Kinematic model of thrust-fault propagation and frontal ramp development (after Dahlstrom 1970, Royse *et al.* 1975, Elliott & Johnson 1980, Boyer & Elliott 1982, Hossack 1983).

To quantify the mechanics in Fig. 5, let us consider the case where such cross-sections are located at a considerable distance from connecting transverse structures such as lateral ramps and tear faults, whereby the deformation can be approximated as plane strain deformation in the plane of the cross-section. From the standpoint of mechanics, the coupling effect between a frontal ramp and a transverse structure, along a cross-section near their juncture, would constitute a more complicated follow-up problem for subsequent analysis if warranted.

On this basis, suppose that the hangingwall of the thrust sheet temporarily becomes locked, say by folding above the frontal ramp in Fig. 5. The ensuing concentration of 'tectonic' compression in the locked region of the pre-existing frontal ramp may produce two effects: (1) shear fracturing and small-scale ramping within the pre-existing ramp region (e.g. compare cross-sections of Serra 1977, and of Suppe 1983), and (2) an increase in the average shear stress along the 'developing thrust'. When this shear stress reaches the critical value P, a rapid transient stress drop occurs from P to S along rupture length L of the 'developing thrust'. This regimen is repeated by renewed concentration of 'tectonic' compression in the locked region of the pre-existing frontal ramp. Therefore, one of the possible modes of deformation in the prospective ramp region is as follows. Recurring stick-slip of the fault block segment designated by L induces shear fracturing in the frontal zone, leading to the formation of the new frontal ramp designated by the short arrows in Fig. 5.

A quantitative solution of this problem in preliminary form yields equations that are almost precisely the same as those obtained by Elliott (1976a, eqns 8, p. 856) in his analysis of an entire thrust sheet. The difference here is that the equations are applied to the fault block segment bounded by the vertical dashed lines in Fig. 5. His equations (8) also can be applied in this manner because an important part of his derivation is based on an Airy stress function; e.g. two-dimensional solutions of Airy stress function problems are independent of scale (Timoshenko & Goodier 1951, p. 25). A detailed expla-

nation of the derivation will be included in the subsequent publication on the general solution of the coupled oscillator problem. The objective of the current discussion is to illustrate qualitatively the role of the parameters responsible for the spacing of the frontal ramps in Fig. 5. Therefore, it is convenient to refer directly to Elliott's equations (8). When σ_{12} of his basal shear stress equation approaches P, we have

$$P \approx \rho g H\left(\sin \alpha + \frac{\kappa H \cos \alpha}{L}\right), \qquad (8)$$

where

α = topographic slope angle
L = rupture length = ramp spacing
$\kappa = C/\rho g H$

in which

C = tectonic compression
ρ = density
g = gravitational acceleration

and

H = thickness of the fault block segment, measured as shown in Fig. 1.

Equation (8) of this paper establishes a relation between the topographic slope, thickness of the fault block segment, and ramp spacing for appropriate values of C and P. Suppose for example that surficial erosion compensates for the structural thickening shown at the 'pre-existing' ramp in Fig. 5. Then an important feature emerges from eqn (8) when we note that the thickness of the thrust belt decreases towards the foreland. If P, κ and α can be treated as nearly constant parameters in certain field areas, then this equation would predict that the ramp spacing decreases toward the foreland. Thus, the model would be consistent with the result of palinspastic analysis reported by Wiltschko & Dorr (1983). However, further analysis of this important problem is required before the reasons for various types of ramp spacing can be determined adequately.

CONCLUDING REMARKS

If the quantitative models described here are developed further, and continue to prove fruitful, then new suites of available data eventually will have to be collected and analyzed. The effect of anisotropy on the structural development of thrust sheets, in response to contrasts in competency and facies changes, would have to be characterized by quantitative parameters beyond those currently employed. For example, a method for processing velocity data of stratigraphic units would have to be explored and developed, with the objective of providing input parameters required for the type of calculations illustrated in this paper. A possible empirical relation between formation velocity and thrust-fault length along-strike already has been indicated in the Southern Canadian foreland belt (see slides 56 and 57 in Verrall *et al.* 1981).

Acknowledgements—Helpful comments on a preliminary version of this paper were made by Peter Geiser (U. Conn.), James Granath and David Weinberg (Conoco, Inc.), Win Means (SUNY, Albany), Sandro Serra (Amoco, Inc.), Carol Simpson (V.P.I.), Steve Wojtal (Oberlin College) and Nick Woodward (U. Tenn.). John Delphia (Boston College) provided assistance with palinspastic analyses of several cross-sections of the Utah–Idaho–Wyoming belt. Acknowledgment is made to the donors of the Petroleum Research Fund, administered by the American Chemical Society, and to Conoco Inc., for partial support of this research.

REFERENCES

Aki, K. 1984. Asperities, barriers, characteristic earthquakes and strong motion prediction. *J. geophys. Res.* **89**, 5867–5872.

Armstrong, F. C. & Oriel, S. S. 1965. Tectonic development of Idaho–Wyoming thrust belt. *Bull. Am. Ass. Petrol. Geol.* **49**, 1847–1866.

Axen, G. J. 1984. Thrusts in the eastern Spring Mountains, Nevada: geometry and mechanical implications. *Bull. geol. Soc. Am.* **95**, 1202–1207.

Bombolakis, E. G. 1979. Some constraints and aids for interpretation of fracture and fault development. Proc. 2nd Int. Conf. Basement Tectonics (edited by Podwysocki, M. H. & Earle, J. S.), Denver, 289–305.

Bombolakis, E. G. 1981. Analysis of a horizontal catastrophic landslide. In: *Mechanical Behavior of Crustal Rocks, The Handin Volume* (edited by Carter, N. L., Friedman, M., Logan, J. M. & Stearns, D. W.), *Geophys. Monogr. Am. geophys. Un.* **24**, 251–257.

Bombolakis, E. G. 1982. Overthrust mechanism and origin of a tectonic ramp in a foreland thrust belt. *Trans. Am. geophys. Un.* (EOS) **63**, 1115.

Bombolakis, E. G., Hepburn, J. C. & Roy, D. C. 1978. Fault creep and stress drops in saturated silt-clay gouge. *J. geophys. Res.* **83**, 818–829.

Boyer, S. E. 1978. Structure and origin of the Grandfather Mountain window, North Carolina. Ph.D. thesis, Johns Hopkins University.

Boyer, S. E. & Elliott, D. 1982. Thrust systems. *Bull. Am. Ass. Petrol. Geol.* **66**, 1196–1230.

Brock, W. G. & Engelder, T. 1977. Deformation associated with the movement of the Muddy mountain overthrust in the Buffington window, southeastern Nevada. *Bull. geol. Soc. Am.* **88**, 1667–1677.

Bustin, R. M. 1983. Heating during thrust faulting in the Rocky Mountains: friction or fiction? *Tectonophysics* **95**, 309–328.

Butler, R. W. H. 1982. The terminology of structures in thrust belts. *J. Struct. Geol.* **4**, 239–245.

Chapple, W. M. 1978. Mechanics of thin-skinned fold-and-thrust belts. *Bull. geol. Soc. Am.* **89**, 1189–1198.

Coppersmith, K. J. & Schwartz, D. P. 1984. Introduction to the special section on fault behavior and the earthquake generation process. *J. geophys. Res.* **89**, 5669–5673.

Dahlstrom, C. D. A. 1970. Structural geology in the eastern margin of the Canadian Rocky Mountains. *Bull. Can. Petrol. Geol.* **18**, 332–406.

Davis, D., Suppe, J. & Dahlen, F. A. 1983. Mechanics of fold-and-thrust belts and accretionary wedges. *J. geophys. Res.* **88**, 1153–1172.

Den Hartog, J. P. 1956. *Mechanical Vibrations*. McGraw-Hill, New York.

Dixon, Joe S. 1982. Regional structural synthesis, Wyoming salient of western overthrust belt. *Bull. Am. Ass. Petrol. Geol.* **66**, 1560–1580.

Delphia, J. G. & Bombolakis, E. G. 1985. Sequential development of a frontal ramp, imbricates, and a major fold in the Kemmerer locale of the Wyoming thrust belt. 34th *A. Mtg SE Sect.* geol. Soc. Am. **17**, 87.,

Donath, F. A. 1968. Role of experimental rock deformation in dynamic structural geology. In: *Rock Mechanics Seminar*, Volume two (edited by Riecker, R. E.), 355–437, Accession No. AD669376, National Technical Information Service, Springfield, Virginia 22161.

Douglas, R. J. W. 1950. Callum Creek, Langford Creek, and Gap map areas, Alberta. *Geol. Surv. Can. Mem.* **225**, 1–124.

Elliott, D. 1976a. The motion of thrust sheets. *J. geophys. Res.* **81**, 949–963.

Elliott, D. 1976b. The energy balance and deformation mechanisms of thrust sheets. *Phil. Trans. R. Soc.* **A282**, 289–312.

Elliott, D. 1980. Mechanics of thin-skinned fold-and-thrust belts: discussion. *Bull. geol. Soc. Am.* **91**, 185–187.

Elliott, D. & Johnson, M. R. W. 1980. The structural evolution of the northern part of the Moine thrust zone. *Trans. R. Soc. Edinb., Earth Sci.* **71**, 69–96.

Fisher, M. W. & Coward, M. P. 1982. Strains and folds within thrust sheets: an analysis of the Heilam Sheet, Northwest Scotland. *Tectonophysics* **88**, 291–312.

Friedman, M., Logan, J. M. & Rigert, J. A. 1974. Glass-indurated quartz gouge in sliding-friction experiments on sandstone. *Bull. geol. Soc. Am.* **85**, 937–942.

Gretener, P. E. 1972. Thoughts on overthrust faulting in a layered sequence. *Bull. Can. Petrol. Geol.* **20**, 583–607.

Gretener, P. E. 1977. On the character of thrust faults with particular reference to the basal tongues. *Bull. Can. Petrol. Geol.* **25**, 110–122.

Gretener, P. E. 1981. Pore pressure, discontinuities, isostasy and overthrusts. In: *Thrust and Nappe Tectonics* (edited by McClay, K. R. & Price, N. J.). *Spec. Publs geol. Soc. Lond.* **9**, 33–39.

Handin, J. 1966. Strength and ductility. In: *Handbook of Physical Constants* (edited by Clark, S. P., Jr.). *Mem. geol. Soc. Am.* **97**, 223–289.

Harris, L. D. & Milici, R. D. 1977. Characteristics of thin-skinned style deformation in the southern Appalachians, and potential hydrocarbon traps. *Prof. Pap. U.S. Geol. Surv. Prof. Pap.* **108**.

Hobbs, B. E., Means, W. D. & Williams, P. F. 1976. *An Outline of Structural Geology*. Wiley, New York.

Hossack, J. R. 1983. A cross-section through the Scandinavian Caledonides constructed with the aid of branch-line maps. *J. Struct. Geol.* **5**, 103–111.

Kasahara, K. 1981. *Earthquake Mechanics*. Cambridge University Press, London.

Knipe, R. J. 1985. Footwall geometry and the rheology of thrust sheets. *J. Struct. Geol.* **7**, 1–10.

Lamerson, P. R. 1982. The Fossil Basin and its relationship to the Absaroka thrust system, Wyoming and Utah. In: *Geologic Studies of the Cordilleran Thrust Belt*, Volume I (edited by Powers, R. B.), Rocky Mountain Association of Geologists, Denver, Colorado, 279–340.

Mandl, G. & Shippam, G. K. 1981. Mechanical model of thrust sheet gliding and imbrication. In: *Thrust and Nappe Tectonics* (edited by McClay, K. R. & Price, N. J.). *Spec. Publs geol. Soc. Lond.* **9**, 79–98.

Morse, J. 1977. Deformation in the ramp region of overthrust faults: experiments with small-scale rock models. In: *Rocky Mountain Thrust Belt Geology and Resources* (edited by Heisey, E. L., Lawson, D. E., Norwood, E. R., Wach, P. H. & Hale, L. A.). Joint Wyoming–Montana–Utah Geological Associations Guidebook, Wyoming Geological Association, 457–470.

Nadai, A. 1950. *Theory of Flow and Fracture of Solids*. McGraw-Hill, New York.

Nelson, R. A. 1981. A discussion of the approximation of subsurface (burial) stress conditions in laboratory experiments. In: *Mechanical Behavior of Crustal Rocks, The Handin Volume* (edited by Carter, N. L., Friedman, M., Logan, J. M. & Stearns, D. W.). *Geophys. Monogr. Am. geophys. Un.* **24**, 311–321.

Nettleton, L. L. 1940. *Geophysical Prospecting for Oil*. McGraw-Hill, New York.

Perry, W. J., Roeder, D. H. & Lageson, D. R. (Eds) 1984. *North American Thrust-Faulted Terranes*. Reprint Series No. 27. Am. Ass. Petrol. Geol., Tulsa, Oklahoma.

Price, R. A. 1981. The Cordilleran foreland thrust and fold belt in the southern Canadian Rocky Mountains. In: *Thrust and Nappe Tectonics* (edited by McClay, K. R. & Price, N. J.). *Spec. Publs geol. Soc. Lond.* **9**, 427–448.

Price, R. A. 1973. Large-scale gravitational flow of supracrustal rocks, southern Canadian Rockies. In: *Gravity and Tectonics* (edited by DeJong, K. A. & Scholten, R.). Wiley, New York, 491–502.

Raleigh, B. 1982. A strategy for short-term prediction of earthquakes. *Bull. Seism. Soc. Am.* **72**, 5337–5342.

Raleigh, B., Healy, J. H. & Bredehoeft, J. D. 1976. An experiment in earthquake control at Rangeley, Colorado. *Science, Wash.* **191**, 1230–1237.

Ramsay, J. G. 1981. Tectonics of the Helvitic nappes. In: *Thrust and Nappe Tectonics* (edited by McClay, K. R. & Price, N. J.). *Spec. Publs geol. Soc. Lond.* **9**, 293–309.

Roeder, D. H., Gilbert, O. E. Jr. & Witherspoon, W. D. 1978. Evolution and macroscopic structure of Valley and Ridge thrust belt, Tennessee and Virginia. Studies in Geology 2. Department of Geological Sciences, University of Tennessee.

Royce, F. Jr., Warner, M. A. & Reese, D. L. 1975. Thrust belt structural gometry and related stratigraphic problems, Wyoming–Idaho–northern Utah. In: *Symposium on Drilling Frontiers of the Central Rocky Mountains* (edited by Bolyard, D. W.). Rocky Mountain Association of Geologists, Denver, 41–54.

Rubey, W. W. & Hubbert, M. K. 1959. Role of fluid pressure in mechanics of overthrust faulting—II. *Bull. geol. Soc. Am.* **70**, 167–206.

Scholz, C. H. 1982. Scaling laws for large earthquakes: consequences for physical models. *Bull. Seism. Soc. Am.* **72**, 1–14.

Schwartz, D. P. & Coppersmith, K. J. 1984. Fault behavior and characteristic earthquakes: examples from the Wasatch and San Andreas fault zones. *J. geophys. Res.* **89**, 5681–5698.

Scott, J. S. & Drever, H. I. 1954. Frictional fusion along a Himalayan thrust. *Proc. R. Soc. Edinb.* **65B** (2), 121–142.

Serra, S. 1977. Styles of deformation in the ramp regions of overthrust faults. In: *Rocky Mountain Thrust Belt Geology and Resources* (edited by Heisey, E. L., Lawson, D. E., Norwood, E. R., Wach, P. H. & Hale, L. A.). Joint Wyoming–Montana–Utah Geological Associations Guidebook, Wyoming Geological Association, 487–498.

Sibson, R. H. 1975. Generation of pseudotachylyte by ancient seismic faulting. *Geophys. J. R. astr. Soc.* **43**, 775–794.

Sibson, R. H. 1977. Fault rocks and fault mechanisms. *J. geol. Soc. Lond.* **133**, 191–213.

Sibson, R. H. 1981. Fluid flow accompanying faulting: field evidence and models. In: *Earthquake Prediction, An International Review* (edited by Simpson, D. W. & Richards, P. G.). Maurice Ewing Series *Am. geophys. Un.* **6**, 593–603.

Sibson, R. H. 1984. Roughness at the base of the seismogenic zone: contributing factors. *J. geophys. Res.* **89**, 5791–5799.

Spang, J. H. & Brown, S. P. 1981. Dynamic analysis of a small imbricate thrust and related structures, Front Ranges, Southern Canadian Rocky Mountains. In *Thrust and Nappe Tectonics* (edited by McClay, K. R. & Price, N. J.). *Spec. Publs geol. Soc. Lond.* **9**, 143–149.

Spang, J. H., Wolcott, T. L. & Serra, S. 1981. Strain in ramp region of two minor thrusts, Southern Canadian Rocky Mountains. In: *Mechanical Behavior of Crustal Rocks, The Handin Volume* (edited by Carter, N. L., Friedman, M., Logan, J. M. & Stearns, D. W.). *Geophys. Monogr. Am. geophys. Un.* **24**, 243–250.

Stockmal, G. S. 1983. Modeling of large-scale accretionary wedge deformation. *J. geophys. Res.* **88**, 8271–8287.

Suppe, J. 1983. Geometry and kinematics of fault-bend folding. *Am. J. Sci.* **283**, 648–721.

Timoshenko, S. & Goodier, J. N. 1951. *Theory of Elasticity*. McGraw-Hill, New York.

Trümpy, R. 1973. The timing of orogenic events in the Central Alps. In: *Gravity and Tectonics* (edited by DeJong, K. A. & Scholten, R.). Wiley, New York, 229–251.

Verrall, P., Dahlstrom, C. & Freund, H. 1981. Structural Geology in the Canadian Overthrust Belt. AAPG continuing education course. Am. Ass. Petrol. Geol., Tulsa, Oklahoma.

Wiltschko, D. V. & Eastman, D. J. 1983. Role of basement warps and faults in localizing thrust fault ramps. *Mem. geol. Soc. Am.* **158**, 177–190.

Wiltschko, D. V. & Dorr, J. A., Jr. 1983. Timing of deformation in overthrust belt and foreland of Idaho, Wyoming and Utah. *Bull. Am. Ass. Petrol Geol.* **67**, 1304–1322.

Winslow, M. A. 1983. Clastic dike swarms and the structural evolution of the foreland fold and thrust belt of the southern Andes. *Bull. geol. Soc. Am.* **94**, 1073–1080.